Integrated approach for the analysis of neonicotinoids in fruits and food matrices

INTEGRATED APPROACH FOR THE ANALYSIS OF NEONICOTINOIDS IN VEGETABLES AND FOOD MATRICES

Paola Calza [a], Barbara Guarino [b], Federica Dal Bello [c*], Anna Dioni [a], Marco Bergero [d] Claudio Medana [c]

[a] Department of Chemistry, University of Torino, via Pietro Giuria 5 - 10125, Torino, Italy. paola.calza@unito.it; anna.dioni@edu.unito.it

[b] Regione Piemonte, Assessorato Agricoltura, Settore Fitosanitario e S.T.C., Laboratorio Agrochimico, Via Livorno, 60 (Palazzina A2 L), 10144 Torino, Italy. barbara.guarino@regione.piemonte.it

[c] Department of Molecular Biotechnology and Health Sciences, University of Turin, via Pietro Giuria 5 - 10125 Torino, Italy. federica.dalbello@unito.it; claudio.medana@unito.it

[d] ASPROMIELE, Via del Passatore 24/C - Fraz. S.Pio, Cerialdo - 12100 – CUNEO. marco.bergero@aspromiele.it

*Corresponding author: federica.dalbello@unito.it

Abstract

We searched for five neonicotenoids (namely acetamiprid, clothianidin, imidacloprid, thiacloprid and thiamethoxam) in 67 samples of fruits, leaves, pollen and honey *via* HPLC-MS by employing QueChERs for extraction and purification. Clothianidin was never detected, while imidacloprid was identified in apple (9.2 µg/kg) and pollen (18-28 µg/Kg), thiacloprid in peaches (21-35 µg/kg) and acetamiprid was identified in the hazel leaves (1266 µg/kg), honey (13-26 µg /Kg) and pollen (11-24 µg/kg). Since the levels found of acetamiprid in hazel, honey and pollen were concerning, we accomplished a study to identify and characterize the possible transformation products via a laboratory simulation. The methodology exploited the analysis by HPLC-HRMS and its application in all matrices. We identify twelve transformation products, whose formation involved dimerization, hydroxylation, oxidation, demethylation and cleavage of the molecule. Three of them were also detected in hazel leaves.

Keywords: neonicotinoids, acetamiprid, transformation products, HPLC-HRMS

1. Introduction

Neonicotinoids belong to one of the most important classes of neurotoxic and systemic synthetic insecticides whose use has increased exponentially over the last three decades since the introduction of the first neonicotinoid, imidacloprid (Jeschke *et al.*, 2008), in 1990. Currently they cover about a quarter of the global market for plant protection (Hervè Thany, 2010). The restrictions imposed on neonicotinoids in Europe were legitimized by emerging knowledge about their impact on the health of bee populations (Demortain, 2021). They act as agonists on nicotinic acetylcholine receptors (nAChRs) by blocking the normal ion exchange action activated by acetylcholine. In insects, the binding to the nAChRs receptors produces repeated losses of charges that cause paralysis and the exhaustion of cellular energy. The great selectivity of neonicotinoids towards the nAChR in insects seems due to the negatively charged moiety containing the nitro or cyano group (Wang *et al.*, 2016). Chloronicotinyl insecticides block nicotinic receptors by inhibiting the passage of nerve impulses, acting mainly by ingestion and are generally absorbed by roots. Their structures guarantee a broad spectrum of action, a low application rate, a rapid absorption and a high selectivity towards insects. Tianicotinyls, second generation neonicotinoids, act by ingestion and contact. They can be absorbed by roots and leaves and also protect newly formed vegetation. Neonicotinoids and related metabolites were detected in plants (Ge *et al*., 2021) and fish food (Serrano *et al*., 2021).

Continuous exposure has shown to cause receptor desensitization and subsequent inhibition of cholinergic neurotransmission, which is still maintained at low concentrations of neonicotinoids due to their high affinity for receptors (Abreu-Villaça *et al.*, 2017). However, the interaction with the receptor may vary in relation to the different chemical substituents and the considered species (Simon-Delso *et al.*, 2015).

In addition to the aforementioned effects, neonicotinoids and their metabolites cause changes in gene expression linked to the functioning of the immune system and loss of orientation, which then lead to an increase in mortality (Furlan *et al.*, 2018). Vertebrate studies have shown that this class of pesticides causes a number of neurological effects on rats, bats and birds, such as reduced memory, decreased cognitive ability and changes in reproduction and the immune system. In the 2000s, diffused bees' deaths occurred and this phenomenon took the name of hive depopulation syndrome (CCD, or Colony Collapse Disorder), whose cause is still unknown. However, some studies have documented the loss of orientation of bees because of

contamination by neonicotinoids, attributable to damage to nerve transmissions closely related to the sight of bees. Due to the damage to the olfactory memory and the reduction in communication among bees through the "waggling dance", a greater difficulty in food supply was noted (Pisa *et al.*, 2015; Okubo *et al.*, 2019). These toxic effects have also been reported for other pollinating insects (Tasman *et al*., 2021). The new European Regulation 2018/785 entered into force on December 2018 and banned the use of Imidacloprid, Clothianidin and Thiamethoxam in open field (Commission implementing Regulation (EU) 2018/785).

Neonicotinoids have a good solubility in water and a low octanol/water partition coefficient (Yamada *et al.*, 1999; da Silva Sousa *et al.*, 2021) that allow their diffusion in large areas thanks to their easiness of transport, with the contamination of plots and water. Once released into the environment, they can persist for long time and can undergo different degradation processes, owing to the action of heat, light, oxygen, carbon dioxide and biological enzymes (Bonmatin *et al.*, 2015; The PPDB Pesticide Properties Database). The persistence of neonicotinoids shows a high variability probably caused by different environmental conditions, the matrix in which they are accumulated and the presence of water.

Despite the large amount of literature focused on the persistence of neonicotinoids, studies on their degradation products and on the neurotoxicity of neonicotinoid metabolites are limited (Sirtori *et al.*, 2014; Voigt *at al.*, 2021). For such, in the present work, we aimed to determine the neonicotinoids together with their transformation products, in order to be able to monitor them in the various matrices. The first step of the work was focused on the targeted search for main neonicotinoids, in particular acetamiprid, imidacloprid, thiamethoxam, clothianidin and thiacloprid, in different food matrices (apple, peach, hazel leaves, honey and pollen). We focused our search on these five compounds included in the Italian regulation. Then possible transformation products (TPs) were produced and characterized by applying a laboratory simulation involving a photocatalytic process. This approach has been already successful applied to river water (Calza *et al.*, 2011; Calza *et al.*, 2013) and biological matrices (Medana *et al.*, 2011) and here we tested it on vegetable matrices for the first time. For the extraction and purification process, the QuEChERS method was used, which is rapidly gaining popularity also for the analysis of pesticides in vegetables and food matrices

(Perestrelo *et al*., 2019). Two complementary mass analyzers were used to perform the analytical determinations. For the targeted approach, a Multiple Reaction Monitoring (MRM) acquisition was utilized on a triple quadrupole tandem mass analyzer. The untargeted study to identify TPs was carried on a High Resolution Mass Spectrometry (HRMS) analyzer (orbitrap).

2. Experimental section

2.1. Materials

Acetamiprid (CAS 160430-64-8 purity ≥ 98.0%), imidacloprid (CAS 138261-41-3 purity ≥ 98.0%), clothianidin (CAS 210880-92-5 purity ≥ 98.0%), thiamethoxam (CAS 153719-23-4 purity ≥ 98.0%), thiacloprid (CAS 111988-49-9 purity ≥ 98.0%), acetonitrile (purity ≥99.9%), methanol (purity ≥99.9%) and formic acid 0.05% (purity 99.9 %) were purchased from Sigma Aldrich. The internal standard used is triphenylphosphate (Sigma Aldrich, purity ≥99.9%).

Sample extraction and purification was performed *via* QuEChERS with UCT QuEChERS 4000 mg $MgSO_4$/ 1000 mg NaCl/ 500 mg sodium citrate buffer, Chromabond QuEChERS Mix VI Diamino/ C18ec Clean-Up-Mix 0,9 g $MgSO_4$, 0,15 g Diamino, 0,15g C18ec, Chromabond QuEChERS Mix III Diamino Clean-Up-Mix 0,9g $MgSO_4$, 0,15g Diamino and Enviroclean ECQUEU615CTB 855mg $MgSO_4$/ 150 mg CUPSA/ 45mg CUCARB.

2.2. Sampling and sample treatment

Fruit and leaves samples were sampled in 67 points spread in the whole Piedmont area. Honey and pollen samplings were carried out in the Piedmont area as part of a multi-year environmental biomonitoring project carried out with bees implemented by Aspromiele, the Piedmont Region and Agrion (Fondazione per la ricerca l'innovazione e lo sviluppo tecnologico dell'agricoltura piemontese) and Figure S1 shows the sampling sites. Fruit and leaf samples were minced with a blender and frozen, while honey and pollen were extracted from the honeycomb. To extract the honey from the honeycomb, the sample was sonicated for a few minutes, while to facilitate the extraction of the pollen the sample was placed in the freezer at -80 °C.

Fruit samples were extracted and purified as follows: 200 µL of triphenylphosphate (10 mg/L) and 10 mL acenonitrile (ACN) were added to 10 grams of fruit and stirred vigorously for 1 min. The citrate buffer salt mix was added, vigorously stirred for 1 min and then centrifuged at 6000 rpm for 15 min. 6 mL were then

withdrawn and dispensed in 15 mL Falcon tubes containing $MgSO_4$ (900 mg) and PSA (15 mg) as d-SPE extracting material, stirred for 1 min, centrifuged at 3000 rpm for 10 min. Successively 4 mL of extract were transferred in glass tubes and added with 40 µL of ACN/5% HCOOH. The extracts were diluted 1:1 with ACN and MilliQ water (1:3) in order to have the same matrix concentration compared to the matrix-matched standards.

The procedure used for leaf samples was the following: 5 grams of sample was weighed and hydrated with 10 mL of MilliQ water. After extraction, the sample was transferred in a Falcon tube containing $MgSO_4$ (900 mg), PSA (150 mg) and GCB as d-SPE phase to eliminate chlorophyll.

As for honey and pollen, the procedure was as follow: 5 grams of honey or 2.5 grams of pollen were weighed and dissolved in 10 mL of MilliQ water. After extraction, the samples were placed in a freeze at -80 °C for 1 hour and centrifuged at 3000 rpm for 5 minutes aimed to eliminate contaminations of wax or residual bees. The sample is then transferred in the Falcon tubes containing d-SPE phase: $MgSO_4$ (900 mg), PSA (150 mg) and C18 to eliminate any remaining lipid residues. The calibration curves for each pesticide in all matrices analyzed had $R^2 > 0.998$. Table S1 collects the LOD and LOQ values for the examined analytes for each matrix considered. The recovery tests were carried out on two levels of spiked samples (20 µg/kg and 40 µg/kg) and the obtained results are shown in Table S2.

2.3. Preparation of standard solutions and analytical curve

2.4. Irradiation procedures

The photocatalytic degradation in MilliQ water was carried out in Pyrex glass cells (2.3 cm × 4.0 cm), filled with 5 mL of analyte (20 mg/L) and TiO_2 (400 mg/L) in a suspension kept under magnetic stirring. Samples were irradiated for different times using a sun simulator (Solarbox, CO.FO.ME.GRA., Milano, Italia) equipped with a cut-off filter at 340 nm. After irradiation, samples were filtered through a 0.45 µm filter (Merck Millipore, Milan, Italy) and analyzed with the proper analytical technique.

2.5. Analytical methods

2.5.1. HPLC-MS

The determination of pesticides in the various matrices was carried out by HPLC-MS/MS using a Finnigan Surveyor HPLC interfaced with a TSQ Fortis triple quadrupole mass spectrometer (Thermo Scientific, Milan, Italy) with ESI ionization source used in positive mode. Qualitative and quantitative MRM transition followed for the analytes are listed in table S3. The chromatographic column used was a 150 × 2.1 mm Hypersil gold column with 3 µm diameter particles (Thermo Scientific, Milan, Italy).

The chromatographic separations of pesticides were performed at a flow rate of 300 µL/min, using 0.1% formic acid-ammonium formate 5mM (eluent A) and methanol (eluent B). Gradient elution started with 2% B, increased up to 50% B in 2 min and to 98% in 7 minutes, followed by 3 min of isocratic elution.

The identification of TPs in ultrapure water was performed using an Ultimate 3000 High Performance Liquid Chromatography coupled through an ESI source to a LTQ-Orbitrap mass spectrometer (Thermo Scientific, Bremen, Germany). The chromatographic separation was achieved with a reverse phase C18 column (Gemini NX C18, 150 × 2 mm, 3 µm, 110 Å; Phenomenex, Castel Maggiore, BO, Italy) using 0.1 % formic acid (eluent A) and acetonitrile (eluent B). Gradient separation ramp started with 5% B, increased up to 100% B in 20 minutes and to 100% in 5 minutes; then the column went back to the initial condition. The LC effluent was delivered to ESI ion source using nitrogen both as sheath and as auxiliary gas. Source parameters were set as followed: sheath gas 35 arbitrary unit (arb), auxiliary gas 15 arb, capillary voltage 4.5 kV and capillary temperature 270 °C. Full mass spectra were acquired in positive ion mode in the *m/z* range between 50 and 500, with a resolution of 30k. MS^n spectra were acquired in the range between ion trap cut-off and precursor ion *m/z.* For structural elucidation of TPs structure Xcalibur software [2.1.0sp1.1160] was used on the basis of mass accuracy (<5 ppm) and RDB (ring double bond) index. Accurate *m/*z values and isotopic abundance in full mass scan chromatogram were used to identify elemental composition whereas MS^n fragmentation was used to hypothesize structural modifications. We followed the Shymanski rules (Schymanski *et al.*, 2014) to assign the identification level [ES] for the recognized TPs of acetamiprid. In all cases the levels assigned was level 3.

2.5.2. Method validation parameters

157 The analytical method was validated with reference to the spiked matrices according to the ICH (ICH, 2018)
158 and FDA (FDA, 2001) guidelines.
159 The linearity of the calibration curves was calculated using the DIFF% parameter, and the results were
160 accepted for values no higher than 25%. The selectivity (SELEC%) was evaluated by comparing the
161 chromatogram of six individual blank matrices (QC) samples that were below 30%. The limit of detection
162 (LOD) was determined as three times the signal-to-noise ratio. Accuracy (BIAS%) and precision (relative
163 standard deviation, RDS% of ACC%) of the lower limit of quantification (LLOQ, expressed as the
164 experimentally measured analyte concentration) were evaluated, with the results being no higher than 20%.
165 The intraday (repeatability) precision and accuracy were calculated in QC samples at three different
166 concentrations and were repeated 5 times. The precision and accuracy values were below 15%.
167 Finally, the recovery calculation was done on the basis of the QuEChERS reported procedure.
168 *2.5.3. TOC analyzer*
169 Total organic carbon (TOC) was measured using a Shimadzu TOC-5000 analyzer (Shimadzu, Milan, Italy)
170 (catalytic oxidation on Pt at 680 °C). The calibration was performed using potassium phthalate.
171 *2.5.4. Ion chromatography*
172 Inorganic ions formed during the degradation of the pesticide were identified by ion chromatography analysis
173 using a Dionex chromatograph equipped with a Dionex 40 ED pump, a Dionex 40 ED conductimetric detector.
174 Anions were analyzed with a Dionex Ion Pac AS9-HC 4 × 250 mm column, and Ion Pac ASRS-ULTRA 4 mm
175 conductivity suppressor, using 9 mM Na_2CO_3 as eluent at 1 mL/min and the retention times were 3.65, 5.13,
176 7.9 and 12.38 min for fluoride, nitrate, chloride and sulphate ions, respectively. Ammonium was analyzed
177 with a IonPac CS12A column 250 mm × 4 mm di diameter using 20mM metansulphonic acid as eluent. In this
178 condition ammonium displayed a retention time of 4.7 min.
179 *2.5.5. Acute toxicity analyzer*
180 The acute toxicity of acetamiprid and its degradation products was assessed using a Microtox Model 500
181 toxicity analyzer (Azur, Milan, Italy). The analyses were performed by evaluating the bioluminescence
182 inhibition assay in the marine bacterium *Vibrio fischeri* by monitoring changes in the natural emission of the

183 luminescent bacteria. Freeze-dried bacteria, reconstitution solution, diluent (2% NaCl) and an adjustment
184 solution (non-toxic 22% sodium chloride) were obtained from Azur (Milan, Italy). Samples were tested in a
185 medium containing 2% sodium chloride, and the luminescence was recorded after 5, 15 and 30 min of
186 incubation at 15 °C. Because no substantial differences were found between the three contact times,
187 hereafter the results related to 15 min of contact are reported. The luminescence inhibition percentage was
188 determined by comparing with a non-toxic control.

189 ## 3. Results and discussion

190 ### 3.1. Search for neonicotinoids in vegetables and food matrices

191 We performed the search for five neonicotinoids (namely acetamiprid, clothianidin, imidacloprid, thiacloprid
192 and thiamethoxam) in 67 samples of fruits, leaves, pollen and honey and results are collected in Table 1.
193 Clothianidin was never detected, while imidacloprid was identified in a sample of apple (9.2 µg/kg),
194 thiacloprid was identified in the three samples of peaches at concentrations 21-35 µg/kg and acetamiprid
195 was identified in the hazel leaves at 1266 µg/kg (see table 1).
196 Table 1 shows the results related to honey and pollen sampled from four different sites from March to
197 October 2019 on a monthly basis. Honey and pollen samples were analyzed to monitor them according to
198 the location of the hives. Statistically, bees can pick up to about 2 km from their hive without using pollen for
199 their livelihood; therefore, pollen found inside the honeycomb has a significant variability, due to the point
200 where the bee went to pick.
201 fz

	Sampling date	Acetamiprid (µg/Kg)	Clothianidin (µg/Kg)	Imidacloprid (µg/Kg)	Thiacloprid (µg/Kg)	Thiamethoxam (µg/Kg)
Honey						
Site 1	March	13 ±-0.5	n.d.	n.d.	n.d.	n.d.
	May	21 ± 5	n.d.	n.d.	n.d.	n.d.
	June	5 ± 1	n.d.	n.d.	n.d.	n.d.
	July	n.d.	n.d.	n.d.	n.d.	n.d.
	August	n.d.	n.d.	n.d.	n.d.	n.d.
	September	n.d.	n.d.	n.d.	n.d.	n.d.
	October	n.d.	n.d.	n.d.	n.d.	n.d.
Pollen						
	March	23 ± 0.5	n.d.	n.d.	n.d.	n.d.

Site 1	May	11 ± 0.5	n.d.	n.d.	n.d.	n.d.
	June	33 ± 0.1	n.d.	n.d.	6±2	n.d.
	June	22 ± 2	n.d.	n.d.	n.d.	n.d.
	July	n.d.	n.d.	n.d.	n.d.	n.d.
Site 2	March	n.d.	n.d.	27± 5	n.d.	n.d.
	April	n.d.	n.d.	18 ± 0.1	n.d.	n.d.
	May	n.d.	n.d.	n.d.	n.d.	n.d.
	June	n.d.	n.d.	27 ± 0.1	n.d.	n.d.
	July	n.d.	n.d.	n.d.	n.d.	n.d.
Peach (758)	-	n.d.	n.d.	n.d.	21	n.d.
Peach (764)	-	n.d.	n.d.	n.d.	30	n.d.
Apple (765)	-	n.d.	n.d.	9.2	n.d.	n.d.
Peach (773)	-	n.d.	n.d.	n.d.	35	n.d.
Hazel leaves (775)	-	1266	n.d.	n.d.	n.d.	n.d.

Table 1. Pesticides detected in honey and pollen, the concentration is expressed in µg/Kg (n.d., not detectable)

As far as honey samples are concerned, the presence of acetamiprid was detected in one of the sampled sites only (site 1) at concentrations between 13 and 21 µg/Kg in March-May, decreases in June (5 ± 1 µg/Kg) and is no longer revealed from July onward.

In the same site the presence of acetamiprid was also noticed in pollen at a concentration 23 ± 0.5 µg/kg in the period between March and June. Conversely, in site 2 the presence of imidacloprid was verified at concentrations between 18 ± 0.1 and 27 ± 0.1 µg/Kg. The presence of thiacloprid was detected only at trace amount.

3.2. Photoinduced transformation of acetamiprid

In view of the high concentration level detected in several matrices, we applied the laboratory simulation to acetamiprid, aimed to search also for its transformation products in the positive samples. The degradation of acetamiprid was carried out in MilliQ water in the presence of titanium dioxide as a photocatalyst under sun simulated light. The pesticide was easily abated; it exhibited $t_{1/2}$ of 15 minutes and completely disappeared in 60 min. Figure 1 reports the progressive mineralization of acetamiprid assessed by analysing the total organic carbon (TOC) and the release of inorganic ions over time. The degradation proceeded with a fast release of chlorine as chloride ions and it reached the stoichiometric amount after 60 min of irradiation,

while nitrogen was mainly released as ammonium (80%) and to a lesser extent (20%) into nitrate ions, as expected (Calza *et al.*, 2005).

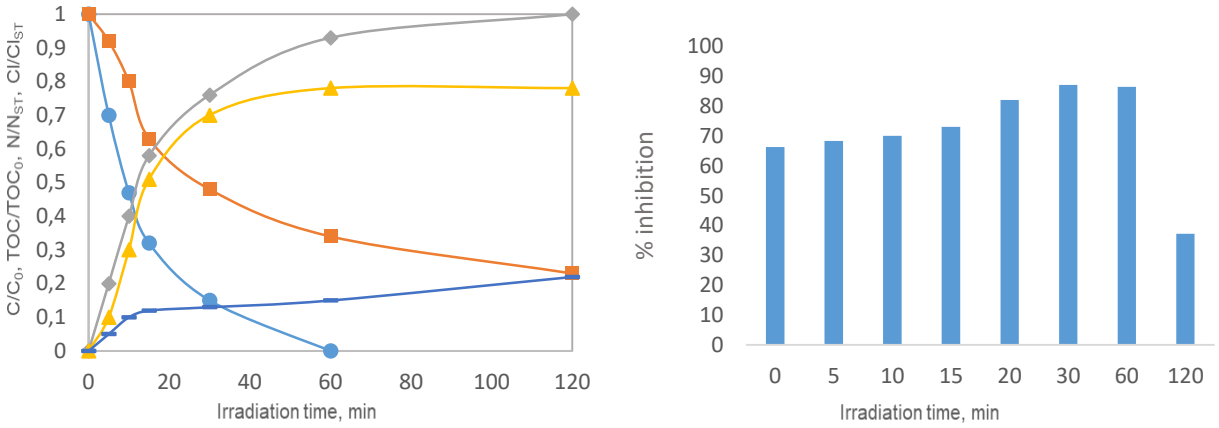

Figure 1. Photocatalyzed transformation of acetamiprid in the presence of TiO_2 as a function of the irradiation time: (left) acetamiprid disappearance (●), TOC (■) and evolution of inorganic ions (chloride (◆), ammonium (▲) and nitrate (-); (right) inhibition percentage as a function of irradiation time.

TOC initially showed a sharp decrease (Guzsvány *et al.*, 2009), but 16 h of irradiation were required to achieve the complete mineralization. Acute toxicity was assessed as well by using *Vibro fischeri* bacteria. Acetamiprid has an EC_{50} 12.66 mg/kg. During the first stages of treatment the inhibition percentage increased, up to 30 min of irradiation (85% of effect), so implying that the transformation involved the formation of TPs more toxic than the parent compound. For longer times, the toxic effect decreased reasonably due to the mineralization of the transformation products responsible for this increase in toxicity.

Along with the degradation of acetamiprid, the photocatalytic degradation led to the formation of 12 transformation products (TPs) identified by HPLC-HRMS with an ESI interface in positive mode. The putative molecular ions were manually identified by the use of a suspect screening list and on the basis of ion abundance on the full mass scan chromatogram. The suspect screening list was compiled exploiting the knowledge of common photocatalysis reactions described in literature (Zhu *et al.*, 2006). The identified transformation products are reported in Table 2, while their evolution profiles over time are collected in Figure 2.

Name	$[M+H]^+$	Empirical formula	Δppm	RT(min)
Acetamiprid	**223.0750**	$C_{10}H_{12}N_4Cl$	2.238	11.12
TP1	**255.0653**	$C_{10}H_{12}O_2N_4Cl$	3.803	10.97
TP2	**253.0935**	$C_{10}H_{12}N_4O_4$	1.456	6.65
TP3	**213.0428**	$C_9H_{10}O_2N_2Cl$	1.259	11.20
TP4	**209.0592**	$C_9H_{10}N_4Cl$	1.671	10.21
TP5	**170.0930**	$C_7H_{12}O_2N_3$	3.509	4.88
TP6	**156.0770**	$C_6H_{10}O_2N_3$	1.582	5.84
TP7	**144.0769**	$C_5H_{10}O_2N_3$	1.020	6.26
TP8	**142.0612**	$C_5H_8O_2N_3$	0.683	5.03
TP9	**128.0816**	$C_5H_{10}ON_3$	-1.862	5.19
TP10	**114.0657**	$C_4H_8ON_3$	-4.282	3.65
TP11	**101.0341**	$C_3H_5O_2N_2$	-4.493	2.45
TP12	**98.0708**	$C_4H_8N_3$	-4.832	5.23

240 **Table 2**. Acetamiprid and its transformation products formed in the presence of TiO_2

241

242 A deep investigation of MS^n fragmentation of the molecule was accomplished aimed to elucidate the

243 structural formulae of TPs. Recorded MS^2 and MS^3 fragments are shown in Table S4.

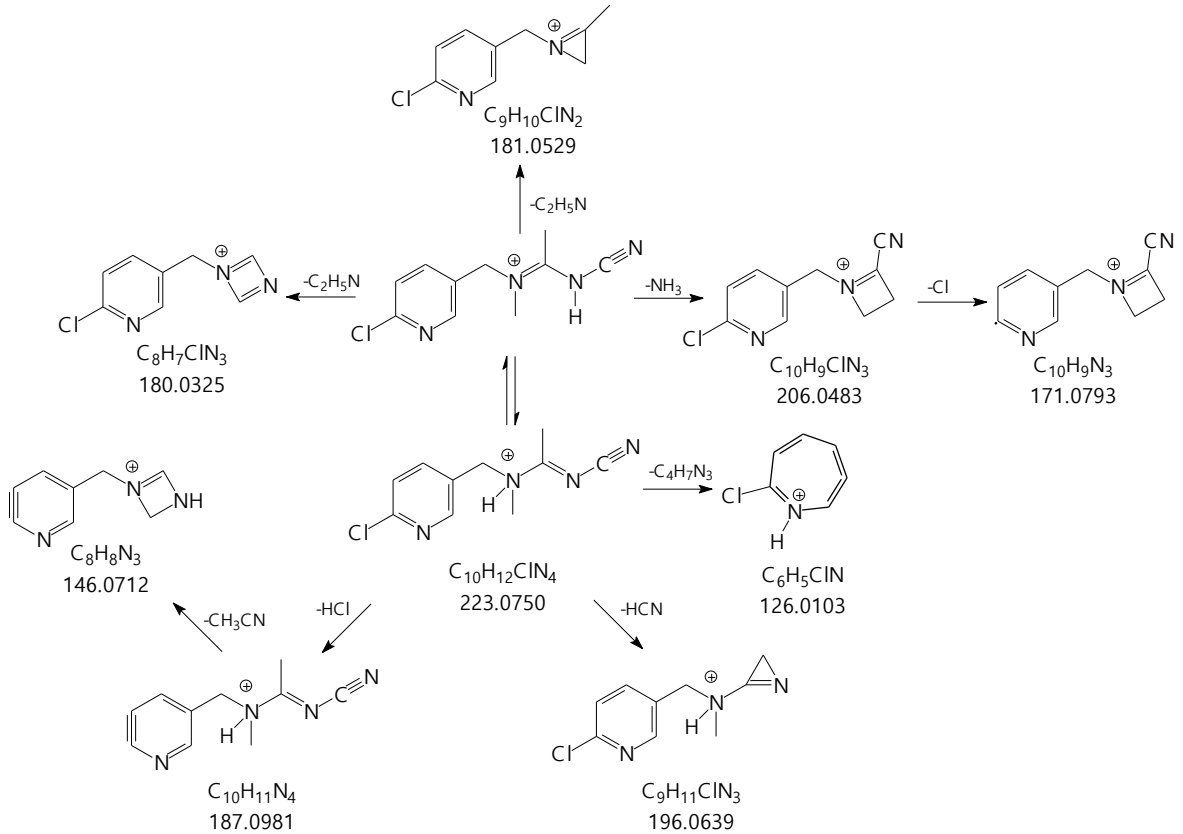

244

245 **Figure 2.** Proposed fragmentation pathways for acetamiprid.

246

The fragmentation of acetamiprid formed the product ion at *m/z* 126.0103 as the base peak, due to the cleavage of the cyano-amidine portion. This ion represented a key fragment for the elucidation of TPs structure. The other product ions involved the loss of HCl from the aromatic ring (187.0981 *m/z)* or the side chain, so bringing to the losses of NH_3 (*m/z* 206.0483*)*, HCN (*m/z* 196.0639*)*, CH_3CN (*m/z* 180.0325) and NH_2CN (*m/z* 181.0529). MS^3 spectra were obtained for two ions: the secondary ion at *m/z* 206.0483 produced the MS^3 ion at *m/z* 171.0793*,* formed via Cl radical loss. The secondary ion *m/z* 187.0981 gave the ion at *m/z* 146.0712 through the loss of CH_3CN.

Table S4 and Figure S2-S11 collects all transformation products together with their MS^2 and MS^3 fragmentation pathways, while all the proposed TPs structures are collected in Scheme 1.

The most abundant TPs were TPs 209, 213 and 98, while TPs 144 and 125 exhibited the faster formation rate reaching the maxima concentration at 5 min.

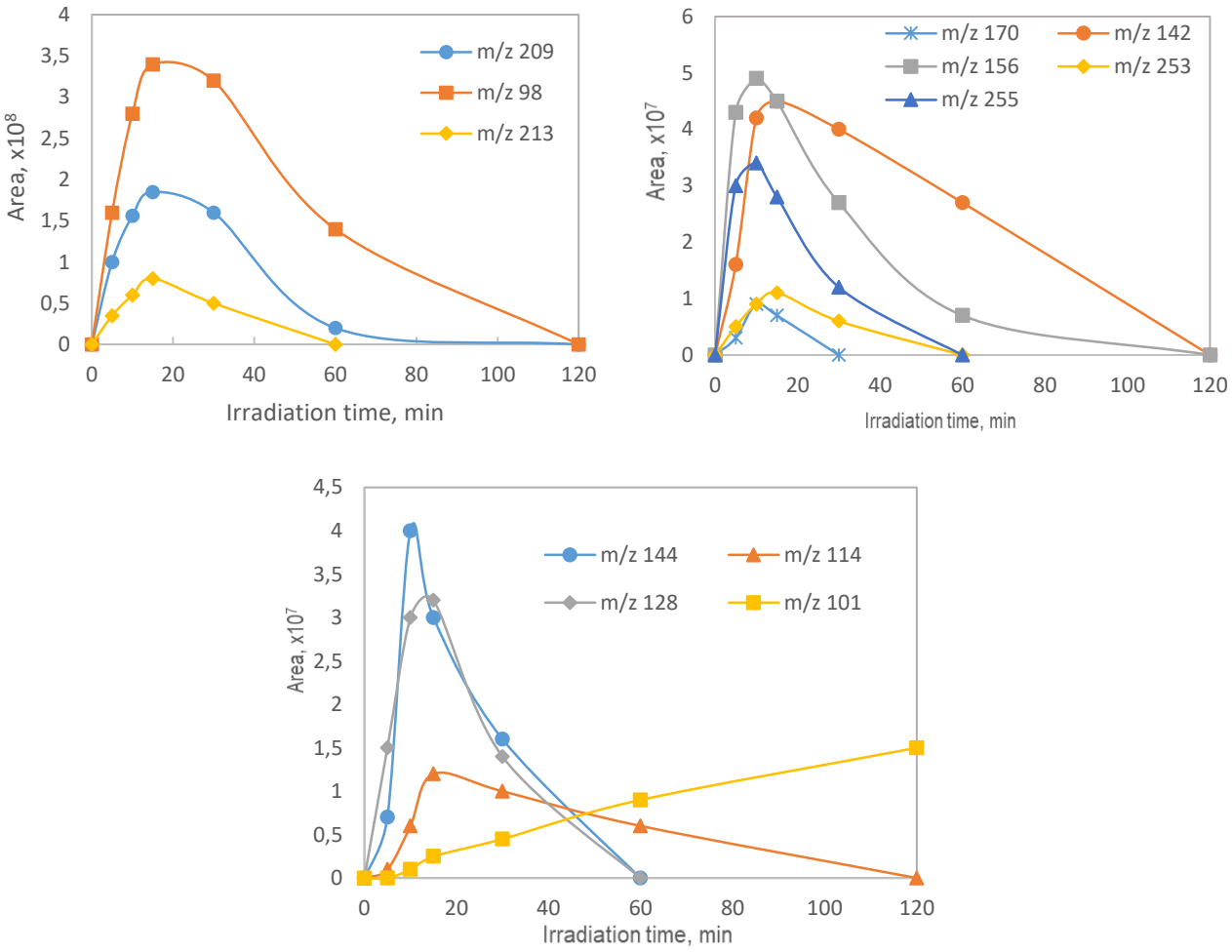

Figure 2. Evolution profiles over time for all TPs detected during the photocatalytic process.

TPs 1-3 underwent hydroxylation or demethylation processes, reached the maximum amount in few minutes and then disappeared within 60 min. The species at *m/z* **255.0653** (TP1) with empirical formula $C_{10}H_{12}O_2N_4Cl$ was attributed to dihydroxy-acetamiprid and it is shown in figure S2. Even if a dihydroxyl-derivative was detected during Fenton reaction, MS^n losses observed in this work accomplished with a different structural attribution (Sirtori *et al.*, 2014). MS^2 spectrum evidenced three structural-diagnostic product ions together with *m/z* 126.0103*,* which accounted for the unmodified chloropyridine ring. The first one, at *m/z* 144.021*,* due to the loss of $C_4H_5ON_3$ allowed locating an OH group on the benzylic position, the second one was *m/z* 169.0165*,* which originated from the loss of $C_3H_6ON_2$ and the third one at *m/z* 157.0527, which involved the amidine cleavage with the loss of $C_3H_2O_2N_2$. The other OH group should be located on one of the two methyl moieties (the only remaining group with hydrogens). MS^3 spectrum of the second generation ion *m/z* 169 generated the product ion at *m/z* 126.0103 through the loss of HCNO and confirmed that one of the two OH groups was on the benzylic carbon.

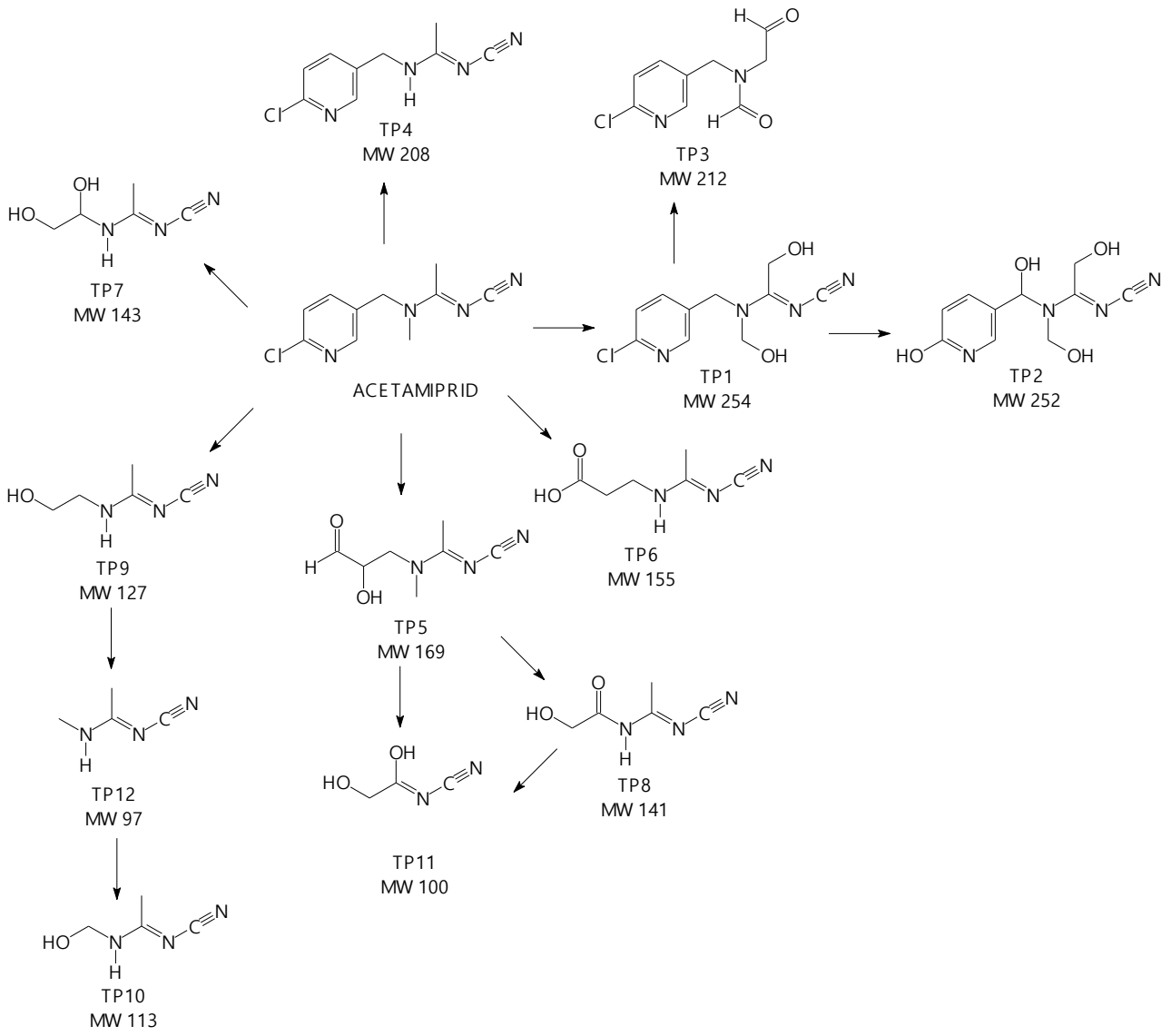

Scheme 1. Proposed transformation pathways for acetamiprid via TiO_2

The TP2 at *m/z* **253.0935** with empirical formula $C_{10}H_{13}O_4N_4$ came from the loss of the chlorine atom and a tetrahydroxylation of the parent molecule. MS^2 spectrum showed the ion at *m/z* 210.0561 formed from the loss of HCNO well-matched with the substitution of chlorine with an OH group. Information were not enough to locate properly the other OH groups, that we indicated similarly to TP1 (see Figure S3).

The formation of a species at *m/z* **213.0428** (TP3) with empirical formula $C_9H_{10}O_2N_2Cl$ involved the detachment of the acetamide moiety and hydroxylation. The presence of the product ion *m/z* 126.0103 allowed excluding a hydroxylation of the aromatic ring and therefore the OH groups were located on the side

chain; the product ion at *m/z* 185.0478 originated from the neutral loss of CO. We explained the water loss accounting from the MS^3 ion at *m/z* 167.0371 by tautomerization of *m/z* 185.0478 (see Figure S4).

The species at *m/z* **209.0592** (TP4) with empirical formula $C_9H_{10}N_4Cl$ involved a demethylation of the parent molecule with the formation of N-(6-chloro-3-pyridyl(methyl)]–N'-cyano-acetamidine. MS^2 spectrum analysis confirmed the identification becouse of the following fragmentaion ions: *m/z* 126.0103, *m/z* 192.0326 (loss of NH_3), *m/z* 182.0482 (loss of HCN), *m/z* 168.0324 (NH_2CN lost) and *m/z* 141.0213 (cleavage of the amidine and the loss of $C_3H_4N_2$). The losses generated were different from those reported in the literature probably becosue of the different MS analyzer (Sirtori *et al.*, 2014) (see figure S5).

All the other TPs derived from the cleavage of the molecule with the detachment of the chloropyridine ring and their disappearance kinetics were quite slower. TPs 170 (TP5) completely disappeared within 30 min, while most of other TPs completely disappeared in 1h, except for TPs 98, 142 and 114 that required 2h and TP 101 that disappeared in 4h.

TP12 at *m/z* **98.0710** with empirical formula $C_4H_8N_3$ was attributed to N-methyl–N'-cyano-acetamidine; it was the most abundant TP and its kinetic profile showed a slow decrease over time. MS^2 spectrum analysis exhibited a product ion at *m/z* 56.0493 formed via the loss of NH_2CN (figure S6) well-matched with literature data (Sirtori *et al.*, 2014; Nicol *et al.*, 2020).

The compound at *m/z* **170.0927** (TP5) with empirical formula $C_7H_{12}O_2N_3$ derived from the cleavage of acetamiprid ring combined with a dihydroxylation and mono oxidation. MS^2 spectrum reported in Figure S7 allowed identifying several structural diagnostic product ions. In particular, the ion at *m/z* 112.0866, which originated from the loss of $C_2H_2O_2$ suggested to locate both oxygenated groups on the terminal side chain. Furthermore, differently from acetamiprid, the product ion at *m/z* 126.0667 had the formula $C_5H_{10}N_3$ and it was the result of the joint loss of H_2O and CO, well matched with the presence of a hydroxyl group and a carbonyl group. An alternative proposal could be a cyclization as described in the photochemical processes (Chen *et al.*, 2018).

TP at *m/z* **142.0611** (TP8) with empirical formulae $C_5H_8O_2N_3$ was probably related to TP5 and TP6. It produced a fragment ion at *m/z* 100.0389. We here described it as hydroxy/cheto derivative but the exact position of the oxygens could be different because of potential isomers (figure S8).

The species at *m/z* **156.0769** (TP6) had the empirical formula $C_6H_{10}O_2N_3$ and involved ring breakdown, demethylation and formation of a carboxylic acid. By observing its MS^2 spectrum shown in figure S9, it generated different product ions, namely *m/z* 110.071 through the loss of formic acid, *m/z* 86.0596 by the concerted loss ow water and cyanogen, *m/z*, 138.0661 which derived from the loss of a H_2O molecule and *m/z* 112.0866, which derived from the loss of CO_2. It was possible to obtain the MS^3 spectrum of the ion *m/z* 138.0661, which generated the product *m/z* 110.071 with the loss of CO. The fragmentation pathway is shown in scheme S9.

TP at *m/z* **128.0816** (TP9) with empirical formula $C_5H_{10}ON_3$ involved demethylation and monohydroxylation. The study of the MS^2 spectrum allowed to identify the ion *m/z* 110.0710*,* which was generated by the loss of a H_2O molecule (figure S10), and it was known from the literature (Dell'Arciprete *et al.*, 2010).

The compound at *m/z* **144.0768** (TP7) with empirical formula $C_5H_{10}O_2N_3$ could derive from the hydroxylation of TP9. The MS^n spectra of the species accounted fot the product ion at *m/z* 126.0660 because of water loss and the subsequent CH_3CN loss giving *m/z* 85.0392 (figure S11).

The transformation product *m/z* **114.0658** (TP10) with empirical formula $C_4H_8ON_3$ can be explained by the hydroxylation of TP 98. MS^2 spectrum exhibited two product ions at *m/z* 96.0552 and 84.0552 respectively formed through the loss of water and formaldehyde. Therefore, the TP10 can be attributed to N-hydroxymethyl–N'-cyano-acetamidine (figure S11).

TP at *m/z* **101.0341** (TP11) with empirical formula $C_3H_5O_2N_2$ derived from a further demethylation and subsequent hydroxylation and could be formed from TPs 114 and 142.

3.3. Search for the TPs acetamiprid in hazel leaves

All TPs identified and characterized so far were searched in the hazel leaf sample since it had the highest concentration of acetamiprid (1266 μg/kg). The sample of leaves underwent the same treatment described

in 2.3 and we detected two of the most abundant TPs identified in the aqueous medium following photocatalysis, namely TPs 209 and 98. The species at 209.0594 *m/z* and 98.0709 *m/z*, whose presence has been found in waters subjected to oxidative degradation process, were identified for the first time in plant or food matrices (Sirtori *et al.*, 2014), even if N-demethylation is a well-known reaction (Chen *et al.*, 2008).

Conclusions

In the present work, some pesticides belonging to the class of neonicotinoids in plant and food matrices have been determined. The determination was made using QuEChERS, an innovative and advantageous extraction and purification method. An analysis method was applied to simultaneously determine all the studied compounds in different matrices. The analysis was carried out with the use of an HPLC-MS/MS and allowed to verify the presence of the analytes considered in 67 real samples of leaves, fruit, pollen and honey.

The work also saw the study of acetamiprid in order to identify and characterize its metabolites and search for them in the matrix. For this purpose, a laboratory simulation was carried out by means of heterogeneous photocatalysis using P25 titanium dioxide as a catalyst.

The identification and characterization of the transformation products were carried out using an HPLC-HRMS/MS analyzer. With the interpretation of the $HRMS^n$ spectra it was possible to identify 12 acetamiprid transformation products. By combining the information relating to the evolution kinetics of the products and the structural characterization, the degradation path of the analyte was hypothesized. It was possible to observe that oxidation was the preferential path of degradation.

The degradation products of acetamiprid were searched in the real sample of hazel leaves. Two metabolites corresponding to those generated because of photocatalytic degradation were identified and confirmed by MS^2 studies. In view of the results obtained, future studies could concern the identification and characterization of the transformation products of other neonicotinoids and their research in environmental matrices.

Authors' contribution

Paola Calza: Conceptualization; Formal analysis; Resources; Writing - Original Draft; Writing - Review & Editing; Supervision; Funding acquisition; Project administration. **Barbara Guarino:** Methodology; Formal

analysis; Validation; Investigation; Supervision; Writing - Review & Editing. **Federica Dal Bello:** Methodology; Formal analysis; Investigation; Writing - Original Draft. **Anna Dioni:** Methodology; Formal analysis; Investigation. **Marco Bergero:** Formal analysis; Investigation. **Claudio Medana:** Formal analysis; Resources; Writing - Review & Editing; Supervision.

References

Abreu-Villaça, Y., & Levin, ED. (2016). Developmental neurotoxicity of succeeding generations of insecticides. *Environment International*, 99, 55-77. https://doi.org/10.1016/j.envint.2016.11.019.

Bonmatin, JM., Giorio, C., Girolami, V., Goulson, D., Kreutzweiser, DP., Krupke, C., Liess, M., Long, E., Marzaro, M., Mitchell, EA., Noome, DA., Simon-Delso, N., & Tapparo, A.(2015) Environmental fate and exposure; neonicotinoids and fipronil. *Environmental Science And Pollution Research International*, 22(1), 35-67. https://doi.org/10.1007/s11356-014-3332-7.

Calza, P., Pelizzetti, E., & Minero, C. (2005) The fate of organic nitrogen in photocatalysis: an overview. *Journal of Applied Electrochemistry*, 35(7), 665–673. https://doi.org/10.1007/s10800-005-1626-7.

Calza, P., Medana, C., Raso, E., Giancotti, V., & Minero, C. (2011). N,N-diethyl-m-toluamide transformation in river water. *The Science Of The Total Environment*, 409(19), 3894–3901. https://doi.org/10.1016/j.scitotenv.2011.06.006.

Calza, P., Medana, C., Padovano, E., Giancotti, V., & Minero, C. (2013). Fate of selected pharmaceuticals in river waters. *Environmental Science And Pollution Research International*, 20(4), 2262–2270. https://doi.org/10.1007/s11356-012-1097-4.

Chen, L., Cai, T., Cheng, C., Xiong, Z., & Ding, D. (2018) Degradation of acetamiprid in UV/H2O2 and UV/persulfate systems: a comparative study. *Chemical Engineering Journal*, 351, 1137–1146. https://doi.org/10.1016/j.cej.2018.06.107.

Chen, T., Dai, Y. J., Ding, J. F., Yuan, S., & Ni, J. P. (2008). N-demethylation of neonicotinoid insecticide acetamiprid by bacterium Stenotrophomonas maltophilia CGMCC 1.1788. *Biodegradation*, 19(5), 651–658. https://doi.org/10.1007/s10532-007-9170-2.

Commission implementing Regulation (EU) 2018/785

Dell'Arciprete, MI., Santos-Juanes, L., Arques, A., Vercher, RF., Amat, AM., Furlong, JP., Mártire, DO., & Gonzalez, MC. (2010) Reactivity of neonicotinoid pesticides with singlet oxygen. *Catalysis Today*, 151, 137– 142. https://doi.org/10.1016/j.cattod.2010.08.001.

Demortain D. (2021). The science behind the ban: the outstanding impact of ecotoxicological research on the regulation of neonicotinoids. *Current opinion in insect science*, 46, 78–82. https://doi.org/10.1016/j.cois.2021.02.017.

da Silva Sousa, J., Oliveira do Nascimento, H., de Oliveira Gomes, H., Ferreira do Nascimento, R. (2021). Pesticide residues in groundwater and surface water: recent advances in solid-phase extraction and solid-phase microextraction sample preparation methods for multiclass analysis by gas chromatography-mass spectrometry, *Microchemical Journal*, 168, 106359. https://doi.org/10.1016/j.microc.2021.106359.

Furlan, L., Pozzebon, A., Duso, C., Simon-Delso, N., Sánchez-Bayo, F., Marchand, PA., Codato, F., Bijleveld van Lexmond, M., & Bonmatin, JM. (2021) An update of the Worldwide Integrated Assessment (WIA) on systemic insecticides. Part 3: alternatives to systemic insecticides. *Environmental Science And Pollution Research International*, 28(10), 11798-11820. https://doi.org/10.1007/s11356-017-1052-5.

Ge, G., Gao, W., Yan, M., Song, W., Xiao, Y., Zheng, P., Peng, C., Cai, H., Hou, R. (2021). Comparation study on the metabolism destination of neonicotinoid and organophosphate insecticides in tea plant (Camellia sinensis L.). *Food chemistry*, 344, 128579. https://doi.org/10.1016/j.foodchem.2020.128579

Guzsvány, VJ., Csanádi, JJ., Lazić, SD., & Gaál, FF. (2009) Photocatalytic degradation of the insecticide acetamiprid on TiO2 catalyst, *Journal of the Brazilian Chemical Society*, 20, 152–159. https://doi.org/10.1590/S0103-50532009000100023.

Jeschke, P., & Nauen, R. (2008). Neonicotinoids-from zero to hero in insecticide chemistry. *Pest Management Science*, 64(11), 1084-98. https://doi.org/ 10.1002/ps.1631.

Medana, C., Calza, P., Giancotti, V., Dal Bello, F., Pasello, E., Montana, M., & Baiocchi, C. (2011). Horse metabolism and the photocatalytic process as a tool to identify metabolic products formed from dopant substances: the case of sildenafil. *Drug Testing And Analysis*, 3(10), 724–734. https://doi.org/10.1002/dta.334.

Nicol, E., Varga, Z., Vujovic, S., & Bouchonnet, S. (2020). Laboratory scale UV-visible degradation of acetamiprid in aqueous marketed mixtures - Structural elucidation of photoproducts and toxicological consequences. *Chemosphere*, 248, 126040. https://doi.org/10.1016/j.chemosphere.2020.126040.

Okubo, S., Nikkeshi, A., S. Tanaka, C., kimura, K., Yoshiyama, M., Morimoto, N.(2019). Forage area estimation in European honeybees (*Apis mellifera*) by automatic waggle decoding of videos using a generic camcorder in field apiaries. *Apidologie*, 50, 243–252. https://doi.org/10.1007/s13592-019-00638-3

Perestrelo, R., Silva, P., Porto-Figueira, P., Pereira, J., Silva, C., Medina, S., & Câmara, J. S. (2019). QuEChERS - Fundamentals, relevant improvements, applications and future trends. *Analytica Chimica Acta*, 1070, 1–28. https://doi.org/10.1016/j.aca.2019.02.036.

Pisa, LW., Amaral-Rogers, V., Belzunces, LP., Bonmatin, JM., Downs, CA., Goulson, D., Kreutzweiser, DP., Krupke, C., Liess, M., McField, M., Morrissey, CA., Noome, DA., Settele, J., Simon-Delso, N., Stark, JD., Van der Sluijs, JP., Van Dyck, H., & Wiemers, M. (2015) Effects of neonicotinoids and fipronil on non-target invertebrates. *Environmental Science And Pollution Research International,* 22(1), 68-102. https://doi.org/10.1007/s11356-014-3471-x.

Schymanski, E. L., Jeon, J., Gulde, R., Fenner, K., Ruff, M., Singer, H. P., & Hollender, J. (2014). Identifying small molecules via high resolution mass spectrometry: communicating confidence. *Environmental science & technology*, 48(4), 2097–2098. https://doi.org/10.1021/es5002105.

Serrano, J., Kolanczyk, R. C., Blackwell, B. R., Sheedy, B. R., & Tapper, M. A. (2021). In vitro metabolism assessment of thiacloprid in rainbow trout and rat by LC-UV and high resolution-mass spectrometry. *Xenobiotica; the fate of foreign compounds in biological systems*, 51(5), 536–548. https://doi.org/10.1080/00498254.2020.1840658.

433 Simon-Delso, N., Amaral-Rogers, V., Belzunces, LP., Bonmatin, JM., Chagnon, M., Downs, C., Furlan, L.,
434 Gibbons, DW., Giorio, C., Girolami, V., Goulson, D., Kreutzweiser, DP., Krupke, CH., Liess, M., Long, E.,
435 McField, M., Mineau, P., Mitchell, EA., Morrissey, CA., Noome, DA., Pisa, L., Settele, J., Stark, JD.,
436 Tapparo, A., Van Dyck, H., Van Praagh, J., Van der Sluijs, JP., Whitehorn, PR., & Wiemers, M. (2015)
437 Systemic insecticides (neonicotinoids and fipronil): trends, uses, mode of action and metabolites.
438 *Environmental Science And Pollution Research International,* 22(1), 5-34.
439 https://doi.org/10.1007/s11356-014-3470-y.

440 Sirtori, C., Agüera, A., Carra, I., & Sanchéz Pérez, J. A. (2014). Application of liquid chromatography
441 quadrupole time-of-flight mass spectrometry to the identification of acetamiprid transformation
442 products generated under oxidative processes in different water matrices, *Analytical And Bioanalytical*
443 *Chemistry*, 406(11), 2549–2558. https://doi.org/10.1007/s00216-014-7678-y.

444 Tasman, K., Rands, S. A., & Hodge, J. (2021). The Power of Drosophila melanogaster for Modeling
445 Neonicotinoid Effects on Pollinators and Identifying Novel Mechanisms. Frontiers in physiology, 12,
446 659440. https://doi.org/10.3389/fphys.2021.659440.

447 Thany, SH.(2010). Neonicotinoid insecticides: historical evolution and resistance mechanisms. *Advances in*
448 *Experimental Medicine and Biology*,683, 75-83. PMID: 20737790.

449 The PPDB Pesticide Properties Database, http://sitem.herts.ac.uk/aeru/footprint/index2.htm

450 Voigt, M., & Jaeger, M. (2021). Structure and QSAR analysis of photoinduced transformation products of
451 neonicotinoids from EU watchlist for ecotoxicological assessment. *The Science of the total environment*,
452 751, 141634. https://doi.org/10.1016/j.scitotenv.2020.141634

453 Wang, NX., Watson, GB., Loso, MR., & Sparks, TC. (2016). Molecular modeling of sulfoxaflor and
454 neonicotinoid binding in insect nicotinic acetylcholine receptors: impact of the Myzus β1 R81T
455 mutation. *Pest Management Science*, 72(8), 1467-74. https://doi.org/10.1002/ps.4220.

456 Yamada, T., Takahashi, H., & Hatano, R. (1999) A novel insecticide, acetamiprid in nicotinoid insecticides and

the nicotinic acetylcholine receptor pp 149-176, Springer, Izuru Yamamoto John E. Casida eds.

Zhu, M., Ma, L., Zhang, D., Ray, K., Zhao, W., Humphreys, W. G., Skiles, G., Sanders, M., & Zhang, H. (2006). Detection and characterization of metabolites in biological matrices using mass defect filtering of liquid chromatography/high resolution mass spectrometry data. *Drug Metabolism And Disposition: The Biological Fate Of Chemicals*, 34(10), 1722–1733. https://doi.org/10.1124/dmd.106.009241.